

Retrieval of Total Precipitable Water and Cloud Liquid Water Path from Jason-2 AMR Observations

Fuzhong Weng¹, Wei Yu², Ninhai Sun³

1. Satellite Calibration & Data Assimilation Branch/STAR/ NESDIS/NOAA, 5200 Auth Road, Camp Springs, Md 20746

2. Dell Inc. for NOAA 5200 Auth Road, Camp Springs, Md 20746

3. IMIS Inc. for NOAA 5200 Auth Road, Camp Springs, Md 20746

Abstract

Total precipitable water (TPW) and cloud liquid water path (CLW) retrieval algorithms developed for Advanced Microwave Sounding Unit (AMSU) operational missions are applied to Advanced Microwave Radiometer (AMR)'s measurements on board Jason-2. The channel frequency shift issue, from 31.4 GHz in AMSU to 34 GHz in AMR, is replaced by mapping AMR measurements to AMSU using Simultaneous Nadir Overpasses (SNO). The comparison between our AMR retrievals and Centre National d'Etudes Spatiales (CNES) products using original AMR measurements and the comparison between our AMR retrievals and the TPW and CLW retrieved from AMSU's measurements demonstrate a high consistence, particularly in the TPW retrievals. Our analyses show that 1. large TPW values move northward slowly while the intensities get slightly stronger from April to September then move gradually southward with the intensities becoming weaker from October to March; 2. large values are near tropical region and small values near pole regions which reflect more water vapor with high evaporation, more clouds and precipitations in low latitudes and less water vapor with low evaporation, less clouds and precipitations in high latitudes; 3. there are more water vapor with high evaporation, more clouds and precipitation in summer than in winter; 4. there are more CLW over Storm Tracks (North Atlantic, North Pacific), Inter-tropical Convergence Zone (ITCZ) and South Pacific Convergence Zone (SPCZ); 5. the TPW values are about 100 times larger than those of CLW. The global oceanic monthly, seasonal, yearly composite of TPW clearly illustrate characteristic meteorological features which indicate that such method can be adapted for other microwave instruments

with similar frequencies for satellite meteorology applications and satellite climate trend study.

1. Introduction

Water vapor is vital for understanding global hydrologic cycle and dynamics of atmospheric circulation. It impacts atmospheric chemistry, pollution and climate trend monitoring. Total precipitable water (TPW) or total water vapor (TWV) plays a major role to short range weather prediction as precipitation, flash flood and other severe weather are closely related to distribution of water vapor. Clouds are important in the global climate change and weather as clouds control the planetary albedo and are precursor of precipitation. The critical role of clouds in the radiative balance of the Earth is widely recognized. Cloud Liquid Water (CLW) also plays a key role in the transport of energy (latent heat) in the earth-atmosphere system. Among the variables in the cloud radiation interactions and feedback processes, cloud liquid water is identified as one of the most important factors. Researcher and operation forecaster can use CLW to access cloud properties and aircraft icing [Bernstein et al. 2005; Guan et al. 2001].

The measurements of TPW and CLW from observations of Radiosonde (RAOBs), ground based microwave radiometers and research aircrafts have been well documented by previous studies [Pratt 1985; Wade 1994; Guan et al. 2001 and 2002; Cober et al. 1996; Han and Westwater 1995; Solheim et al.1998; Vaillancourt et al.2003; Tremblay et al., 2003]. Many researchers have focused on the retrieval of TPW and CLW by microwave radiometers aboard satellites or on the development of algorithms for different satellites to retrieval TPW and CLW since the

launch of the Special Sensor Microwave Imager (SSM/I) [Alishouse et al. 1990a,b; Ferraro et al. 1996; Grody et al. 2001; Greenwald et al. 1993; Kokhanovsky et al. 2006; Liu and Curry 1993; Weng and Grody 1994a,b; Weng et al. 1997 and 2003; Wentz 1997]. These effects have increased the application of the satellite retrieved TPW and CLW to numerical models [Deblonde and Wagneur 1997] and climate analysis [Jackson and Stephens 1995; Trenberth and Guillemot 1995]. However, not only inter-comparisons between CLW algorithms from different satellites have shown significant differences, but also the retrieved values of CLW using different algorithms have remain large discrepancies because of the difficulty in validating the satellite-derived values of Liquid Water Path (LWP) [Liu and Curry 1993]. It took lots of time, energy and cost for the remote sensing community to develop many new algorithms for different observation platforms with big different results especially for CLW path.

The primary mission of recently launched Jason-2 is to measure sea surface heights for determining ocean circulation, climate change and sea-level rise. The altimetric sea surface height (SSH) measurements are derived from the difference between the orbit altitude of the satellite and the corrected range measurement from the altimeter [Desai and Haines 2004]. One of the largest error sources for the corrected range measurement is the wet troposphere path delay in which total water vapor play a crucial role and cloud liquid water play a smaller role. Since pocket of high humidity can have limited size and travel fast, modeling of these phenomena is extremely difficult. Therefore, most altimeter satellites carry a microwave radiometer that senses the radiation from the earth at two or three distinct frequencies in the range of 18 to 37 GHz, in which absorption by water vapor and liquid water occurs. The measured radiation at these frequencies is expressed in

terms of brightness temperatures (TBs). These TBs can be converted to estimates of total water vapor and liquid water content which in turn determine attenuation and path delay of the altimeter radar pulse. The third radiometer frequency is used to estimate and eliminate the effect of sea surface roughness and foam on the brightness temperatures [Scharroo et al. 2004]. In order to save time and cost, instead of developing another algorithm for TPW and CLW of AMR measurements the operational AMSU water vapor and cloud algorithms of Weng et al. [2003] combined with a linear mapping technique is used to retrieve TPW and CLW simultaneously with brightness temperature measurements from channel 23.8 and 34.0 GHz of Advanced Microwave Radiometer (AMR) on board satellite Jason-2 under Simultaneous Nadir Overpasses (SNO) condition for 95% global unfrozen ocean environment. The combination technique is evaluated by comparing our retrieved TPW and CLW to AMSU-A's retrieved quantities based on traditional well tested 23.8 and 31.4 GHz microwave radiometric retrieval technique for AMSU-A's measurements and also by comparing our retrieved TPW and CLW to same quantities retrieved by CNES based on their technique on the same AMR brightness temperature measurements.

2. Linear Mapping between AMSU-A and AMR under SNO condition

a. Dataset

Advanced Microwave Radiometer (AMR) on board of Jason-2 that was launched on June, 20 2008 is a nadir viewing passive microwave instrument which collects radiation reflected by the oceans at frequencies of 18.7, 23.8 and 34.0 GHz with a spatial resolution near 25 km. In this study, AMR

brightness temperatures at channel 23.8 and 34.0 GHz were used to retrieve total precipitable water and cloud liquid water over oceans for the period spanning from June 22, 2008 to Dec. 31, 2009. The same retrieval procedure can be used for data of other years when all data of other years become available in order to get more accurate mapping coefficients. There are three families of geophysical data records (GDRs) of Jason-2 products in NetCDF format, distinguished by increasing latency and accuracy, going from the operational GDR (OGDR, available 3-5 hours), to the Interim GDR (IGDR available 1-2 days), to the final GDR (available around 60 Days). The final GDR data were used here as it is most completed, accurate and validated data. The data covers the entire Earth between 66.15°S to 66.15°N that is about global 95% unfrozen ocean environment.

b. Inter-satellite Calibration of AMSU-A and AMR Radiometers Using the SNO Method

Simultaneous Nadir Overpass (SNO) uses a novel approach that takes advantage of inter-satellite calibration with SNO observations at the orbital intersections between each succeeding pair of satellites. At each SNO, radiometers from each pair of satellites view the same place at the same time at nadir, thus eliminating uncertainties associated with the atmospheric path, view geometry, and time differences. As a result, uncertainties in the inter-satellite calibration are greatly reduced. This method is useful for the on-orbit verification of instrument performance for newly launched radiometers, calibration transfer from instruments on one satellite to those on another, as well as retrospective analyses of historical data in constructing time series for climate studies [Cao et al. 2005].

In this project, SNO observations contain brightness temperatures from AMR and AMSU-A. Criteria for the SNOs are: 1) at the SNO, the distance

between nadir pixels of two orbits < 20 km; 2) time difference between nadir pixels of the two orbits is less than 5 minutes. A pixel by pixel match is performed for the matchup data between the two satellites based on the latitude and longitude of each pixel.

c. Linear Mapping Technique

Since the first launch of the Advanced Microwave Sounding Unit (AMSU) onboard NOAA-15, the products including cloud liquid, water vapor, rain rate, snow cover and sea ice concentration have been operationally generated by NOAA with a quality similar to those derived from SSM/I although the AMSU only has four window channels. Since AMR has two channels similar to AMSU-A, the operational AMSU water vapor and cloud algorithms can be directly used for AMR after channels are linearly mapped into AMSU-A channels. This linear mapping also calibrates AMR data using AMSU-A as a reference.

AMR on board JASON-2 and AMSU-A of Met-Op Simultaneous Nadir Overpass match up data are imported into excel files to get following linear mapping coefficients and equations from the scattered plot [Figure 1]:

For 2008 data:

$$Y_{amr} = 1.0002X_{amsu-a} \text{ (both AMSU and AMR channels at 23.8 GHz)}$$

$$Y_{amr} = 0.9778X_{amsu-a} \text{ (AMR channel at 34.0 GHz and AMSU at 31.4 GHz).}$$

For 2009 data:

$$Y_{amr} = 0.9991X_{amsu-a} \text{ (both AMSU and AMR channels at 23.8GHz)}$$

$$Y_{amr} = 1.0246X_{amsu-a} \text{ (AMR channel at 34.0 GHz and AMSU at 31.4 GHz).}$$

3. AMR Water Vapor and Cloud Liquid Water Retrievals

a. AMSU-A Water Vapor and Cloud Algorithms

Since in microwave frequencies the radiance is linearly proportional to temperatures, the brightness temperatures are preferred in the algorithm. Using equation (4) of Weng's 2003 paper, the cloud liquid water and total precipitable water can be derived using two AMSU window channels at 23.8 and 31.4 GHz assuming an isothermal atmosphere. Essentially, cloud liquid water (L) and total precipitable water (V) are derived using

$$L = a_0 \mu [\ln(T_s - TB_{31}) - a_1 \ln(T_s - TB_{23}) - a_2]$$

and

$$V = b_0 \mu [\ln(T_s - TB_{31}) - b_1 \ln(T_s - TB_{23}) - b_2],$$

respectively, where T_s is the sea surface temperature and the coefficients are defined in Weng et al. (2003) and are functions of ocean surface wind, surface emissivity, and cloud layer temperature if clouds exist in atmosphere.

b. Total Precipitable Water and Cloud Liquid Water Retrievals

AMR data which includes brightness temperatures with latitude, longitude information from channels 23.8 and 34.0GHz and satellite observation times during the day were extracted from original swath data set then converted to grid data in ascending and descending situations in order to use Gdas grid data and easily compare to AMSU-A data. Surface winds and sea surface temperatures of the auxiliary data required in above

algorithm formula are taken from Global Data Assimilation System (Gdas) which is a grid data from 1° - 360° and 90° S- 90° N with both latitude / longitude resolution at 1 degree. To get the correspondent Gdas data for satellite observation, 4 Gdas files are read simultaneously and interpolated by weight spatially and temporarily according to satellite observation time.

AMR brightness temperatures with correspondent auxiliary Gdas sea surface winds and sea surface temperature data were substituted into AMSU water vapor and cloud retrieval algorithm equations based on above mapping relation to get daily AMR total precipitable water and cloud liquid water data for 2008, 2009 [Figures 2 a, b, d, e]. The monthly averaged TPW and CLW are also computed and plotted [Figure 2 c, f].

4. Preliminary Results and AMR Linear Mapping Algorithm Performance

a. Preliminary Results

TPW were retrieved over ocean only for this study. All daily, monthly, seasonal and yearly TPW maps show the large values near tropical region and small values near pole regions which reflect more water vapor with high evaporation, more clouds and precipitations in low latitudes and less water vapor with low evaporation, less clouds and precipitations in high latitudes. The monthly averaged maps indicate that the large TPW values in red move northward slowly while its intensities get slightly stronger (red areas becoming larger and brighter) from April to September (April 2009 to Sept. 2009 see Figure 3 a, b) then move gradually southward with their intensities becoming weaker from October to March (Oct. 2008 to March 2009 see Figure 3 c, d; Only first and last monthly maps are given here, all

other monthly mean plots are available upon request). We can monitor the location, extent and movement of tropical moisture from these movements which is useful for operation forecaster to do severe weather and precipitation forecast.

The analysis from seasonal maps [Figures 3 e, f] illustrate that more water vapor with high evaporation, more clouds and precipitation in summer than those in winter. There are more TPW in Hudson Bay in summer than in winter. The reddish and brighter areas along 66.15° S are most likely caused by sea ices in those areas. The half year (available upon request) and yearly averaged TPW [Figure 3 g] look similar to those of monthly and seasonal average as Jason-2 satellite passes over the same point on the Earth's surface (to within one kilometer) every ten days.

The relative large values which appear in red on the daily and monthly CLW maps [Figures 2 d,e,f] demonstrate larger amount of cloud water and more convective clouds in those areas and blue and green colors **show** low to moderate amount cloud water or less cloud droplets in the columns from surface to top of the atmosphere in those areas. There are more CLW over Storm Tracks (North Atlantic, North Pacific), Inter-tropical Convergence Zone (ITCZ) and South Pacific Convergence Zone (SPCZ) and more sea ices showing in red and brighter colors along 66.15° S which are consistent with CLW and sea ice pattern retrieved from AMSU-A. The reasons that CLW pattern in the monthly AMR maps are not as obvious as the pattern of TPW and not as clear as CLW pattern of AMSU-A are due to: 1) clouds are naturally spottier and not continuous in the atmosphere and in many places of the world there are no clouds with CLW values at zeros; 2) there are still gaps in the monthly averaged map due to Jason-2 satellite

passing over the same point on the Earth's surface (to within one kilometer) every ten days. CLW is also valid over ocean only with values larger than 0.7mm being not reliable.

It is shown in both monthly mean and daily plots that TPW values are about 100 times those of CLW which means that water content in the column of atmosphere from surface to top is in the order of one hundred time larger in vapor form than in liquid form. This result is in good agreements with those from AMSU-A on board NOAA-KLM and AMSU-A on board of EuMetSat's Met-Op.

b. Linear Mapping Technique Performance

The correlation between AMRus (retrieved with our linear mapping method) and AMSU-A for 08012009 (randomly selected) is at 0.9075 for ascending and 0.9055 for descending in the TPW scattered plot [Figure 4 a, b] after coastal contamination with islands or/and clouds is screened out. The standard deviation of TPW from AMRus subtracting AMSU-A dataset is 9.18993mm for ascending case and 8.75910mm for descending case. The TPW RMS difference between AMRus dataset and AMSU-A dataset is 11.93mm for ascending and 11.41mm for descending which is good considering many TPW values over 70mm.

TPW and CLW retrieved by Centre National d'Etudes Spatiales (CNES) were also extracted from original AMR data set and used to compare to our retrieved TPW and CLW in linear mapping technique with very good agreements: The daily correlations between our retrieved TPW and those of CNES retrieved for 08/01/2009 (randomly selected) are at 0.9751 for ascending and 0.9785 for descending [Figure 4 c,d]. The standard deviation of TPW from AMRus subtracting AMRec (retrieved from CNES)

dataset is 3.02215mm for ascending case and 3.61641mm for descending case. The TPW RMS difference between AMRus dataset and AMRec dataset is 3.625 mm for ascending and 4.291 mm for descending for 08/01/2009 which is very good. The correlations of August of 2009 monthly averaged TPW between our retrievals and theirs are at 0.9815 for ascending and 0.9823 for descending [Figure 4e, f]. However, the correlations are a bit lower when smaller TPW values are included for either daily or monthly correlations.

The CLW correlation between our AMR daily retrieved and CNES AMR retrieved is at 0.8604 for descending and 0.7773 for ascending [Figure 5 a, b] for 08/01/2009 which is better than the CLW correlation between our AMR retrievals to AMSU-A retrievals. The randomly selected CLW correlation values for other days (available upon request) are between 0.7773 to 0.8604. The standard deviation of CLW from AMRus subtracting AMRec dataset is 0.153267mm for descending case and 0.23456mm for ascending case for 08/01/2009. The CLW RMS difference between AMRus dataset and AMRec dataset is 0.15355mm for descending and 0.23798mm for ascending for the same date. Although the CLW correlation is not as good as that of TPW it is still reasonable and realistic considering that CLW is a less continuous and spottier parameter comparing to TPW. The results are in good agreements with those of retrievals [Grody and Weng 2001] that also showed larger variability of CLW in both space and time.

The bias distribution from CLWec subtracting CLWus are plotted [Figure 5 c,d] as histogram which shows the numbers of CLWec-CLWus falling in various ranges from -0.15 to 0.15mm with step increase at 0.01mm. The difference between CLWec and CLWus are plotted on the X axis and their numbers on the Y axis. The histogram indicates that a rough

approximation of the CLWec subtracting CLWus number distribution is near the normal distribution with large numbers located around the center of the distributions.

The CLW is also evaluated qualitatively by plotting cloud cover comparison between our linear mapping retrieval to AMSU-A retrievals and our linear mapping retrievals to CNES retrievals [Figure 5 e, f]. The X-axis is the cloud existence threshold from 0 to maximum CLW here at 2.5 mm. The Y-axis is the percentage of points where both retrievals are higher than the threshold with respect to all retrieved points. It is found between 0.01mm to 0.2mm thresholds both retrievals have the high consistence in cloud existence for both AMRus vs. AMRec and AMRus vs. AMSU-A cases.

5. Summary and Conclusions

The combination of the operational AMSU water vapor and cloud algorithms with a linear mapping technique presented in this paper provides a new tool for retrieval water vapor and cloud liquid water from AMR on board Jason-2 whose primary mission is to measure sea surface heights. Although TPW (or TWV) is a critical factor in achieving highest accuracies in the determination of sea surface height the retrieved TPW and CLW can be used widely in other weather and climate study and applications. Our analyses not only provide some new and interesting results but also make an inter-calibration polar orbiting radiometers between AMR on board Jason-2 and AMSU-A on board Met-Op to achieve the consistency of the climate observations data. In summary the following points are included in this paper:

1. The operational AMSU water vapor and cloud algorithms combined with a linear mapping technique is used to retrieve total precipitable water and cloud liquid water in the Simultaneous Nadir Overpasses (SNO) condition from AMR's measurements for 95% global unfrozen ocean environment.
2. The linear mapping algorithm is evaluated by comparing retrieved TPW and CLW with same quantities retrieved by AMSU-A based on traditional well tested 23.8 and 31.4 GHz microwave radiometric retrieval technique from AMSU-A's measurements and also by comparing our retrieval quantities to TPW and CLW retrieved by CNES based on their technique on the same AMR measurements. The TPW correlations between our retrievals and those retrieved by CNES and between our retrievals and AMSU-A's retrieval are very good. The CLW correlation between our retrieval and CNES retrieval is good and the CLW correlation between our retrieval to AMSU-A retrieval is scattered.
3. Our analyzed results show that the large TPW values near tropical region and small values near pole regions which reflect more water vapor with high evaporation, more clouds and precipitations in low latitudes and less water vapor with low evaporation, less clouds and precipitations in high latitudes.
4. Our analyses from monthly mean plots indicate that the large TPW values move northward slowly while intensities get slightly stronger from April to September then move gradually southward with intensities becoming weaker from October to March.
5. The analysis from season's maps illustrates that more water vapor with higher evaporation, more clouds and precipitation in summer

than in winter. There are more TPW in Hudson Bay in summer than in winter. The reddish and brighter areas along 66.15° S are most likely caused by sea ices in those areas.

6. It is shown in our study that TPW values are about 100 times those of CLW which means that water content in the column of atmosphere from surface to top is in the order of one hundred times larger in vapor form than in liquid form.
7. There are more CLW over Storm Tracks (North Atlantic, North Pacific), Inter-tropical Convergence Zone (ITCZ) and South Pacific Convergence Zone (SPCZ) and more sea ices showing in red and brighter along 66.15° S which are consistent with CLW and sea ice pattern retrieved from AMSU-A.
8. It can be concluded that the combination of the operational AMSU-A water vapor and cloud algorithms with a linear mapping technique under SNO condition is a simple but very efficient and practical retrieval method which can be easily adapted for use in other microwave instruments onboard satellites with similar frequencies in the application of CLW and TPW retrievals for weather and climate study and application

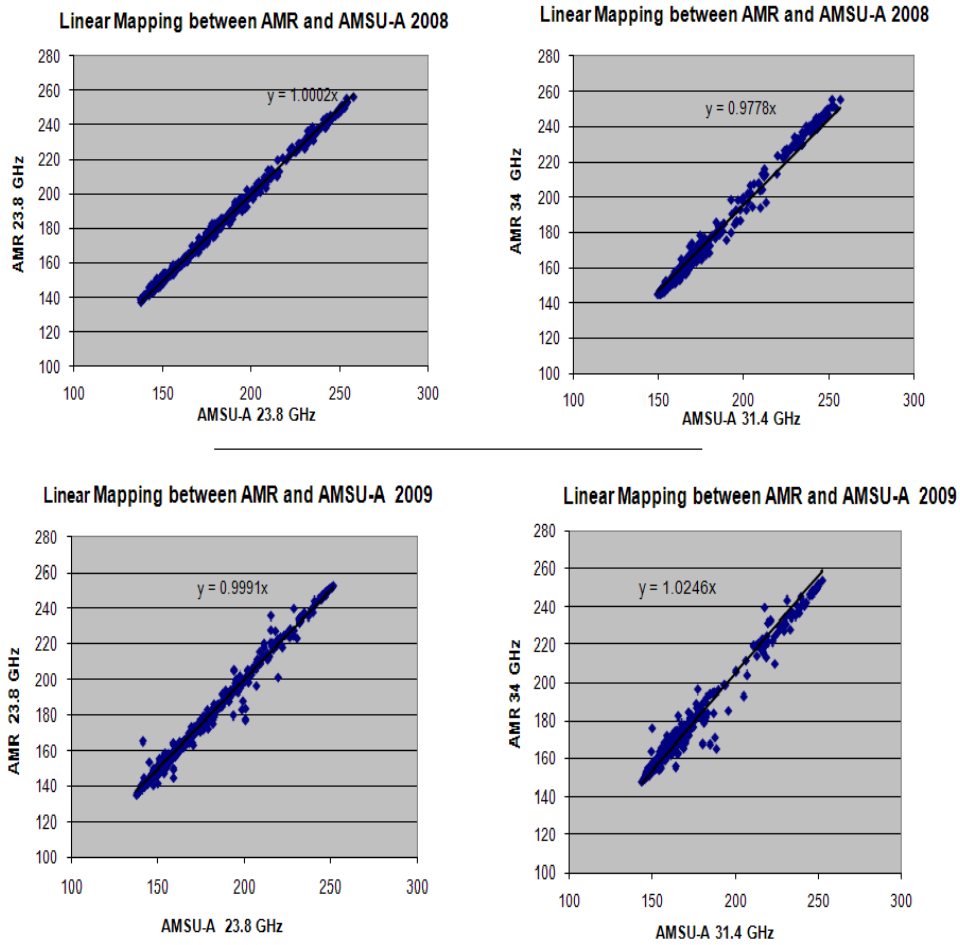


Figure 1 Linear Mapping between AMR and AMSU-A for 2008 and 2009

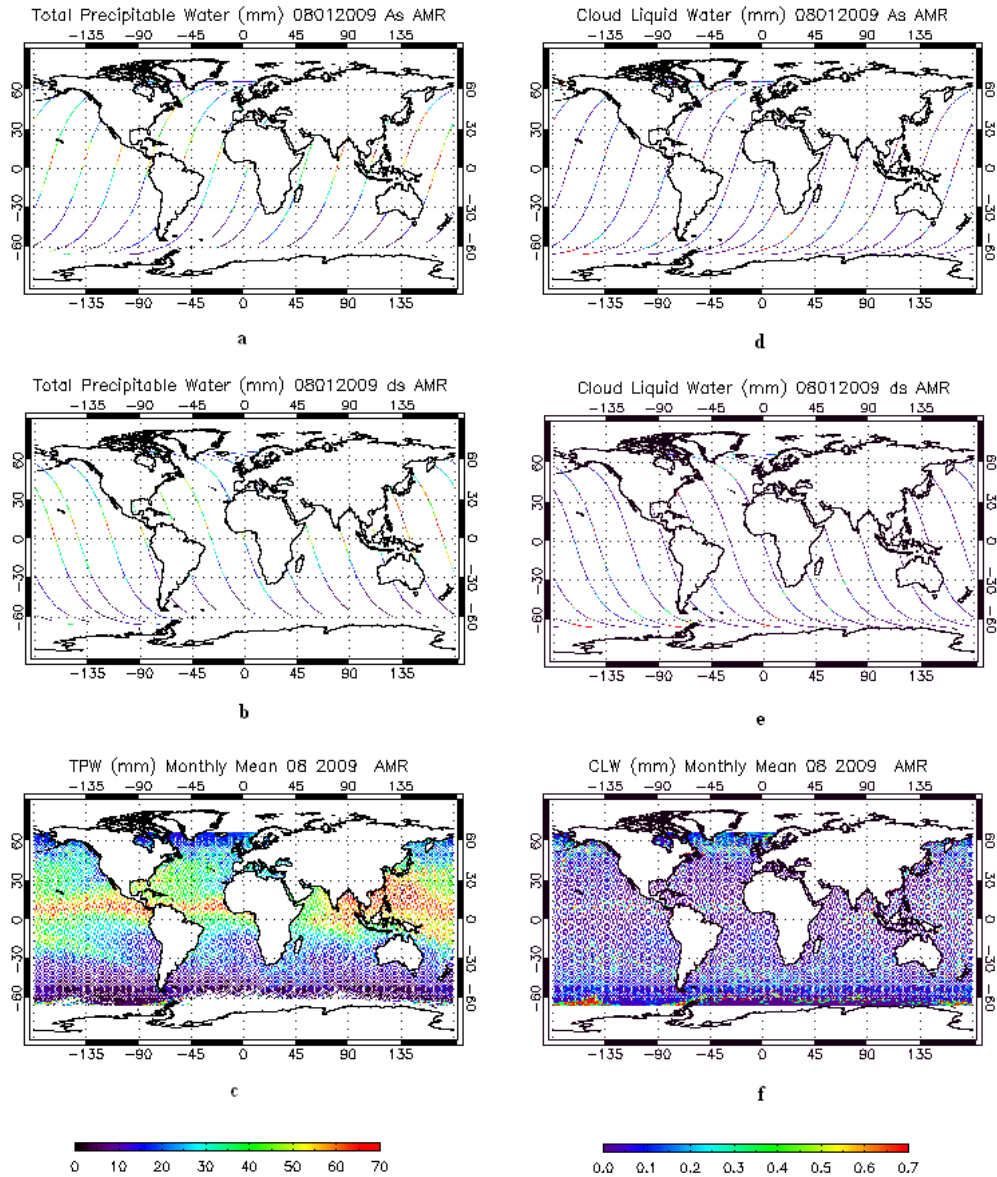


Figure 2 Daily and Monthly Mean Total Precipitable Water (mm) and Cloud Liquid Water (mm)

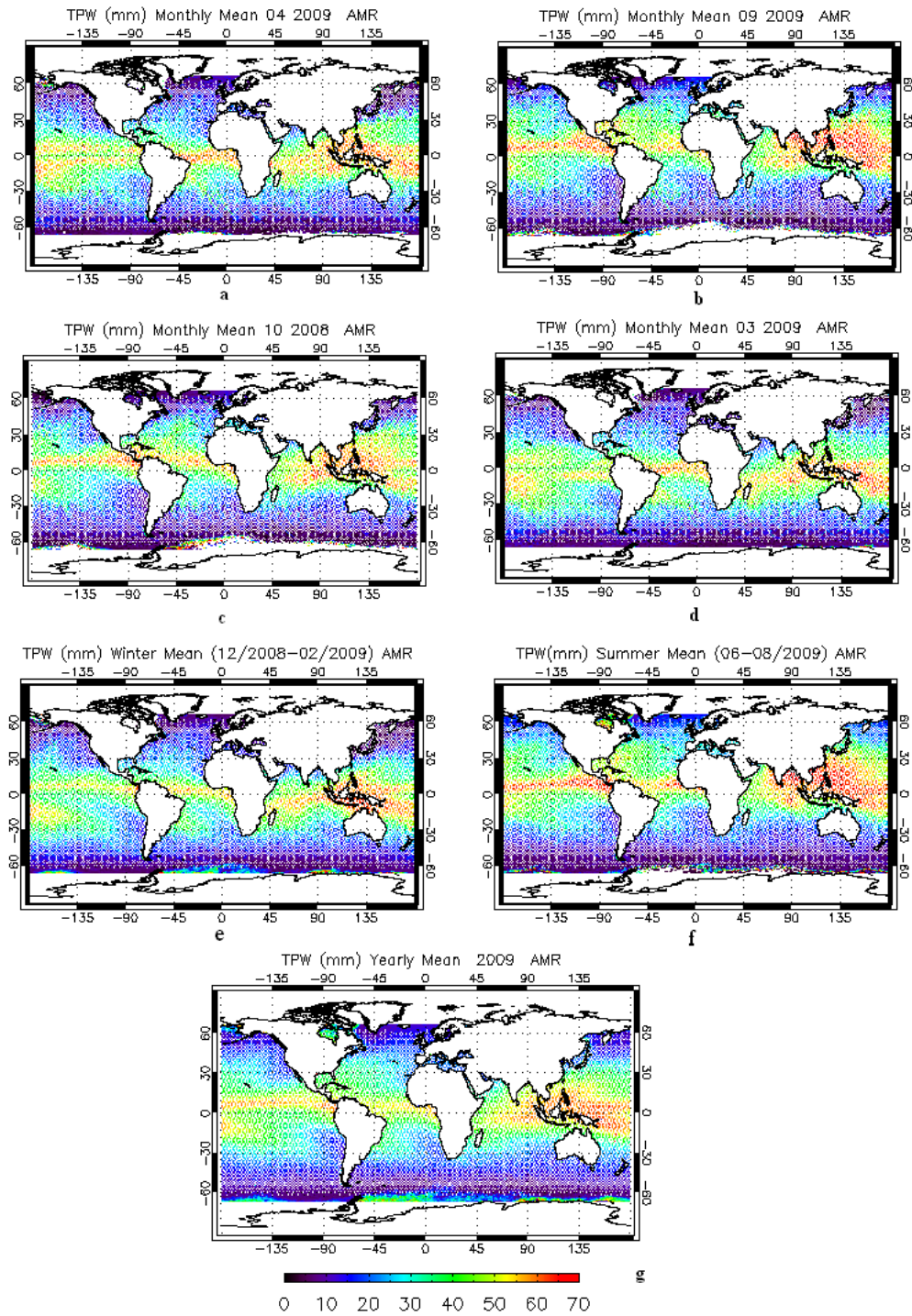


Figure 3 Monthly Seasonal and Yearly Mean Total Precipitable Water (TPW mm)

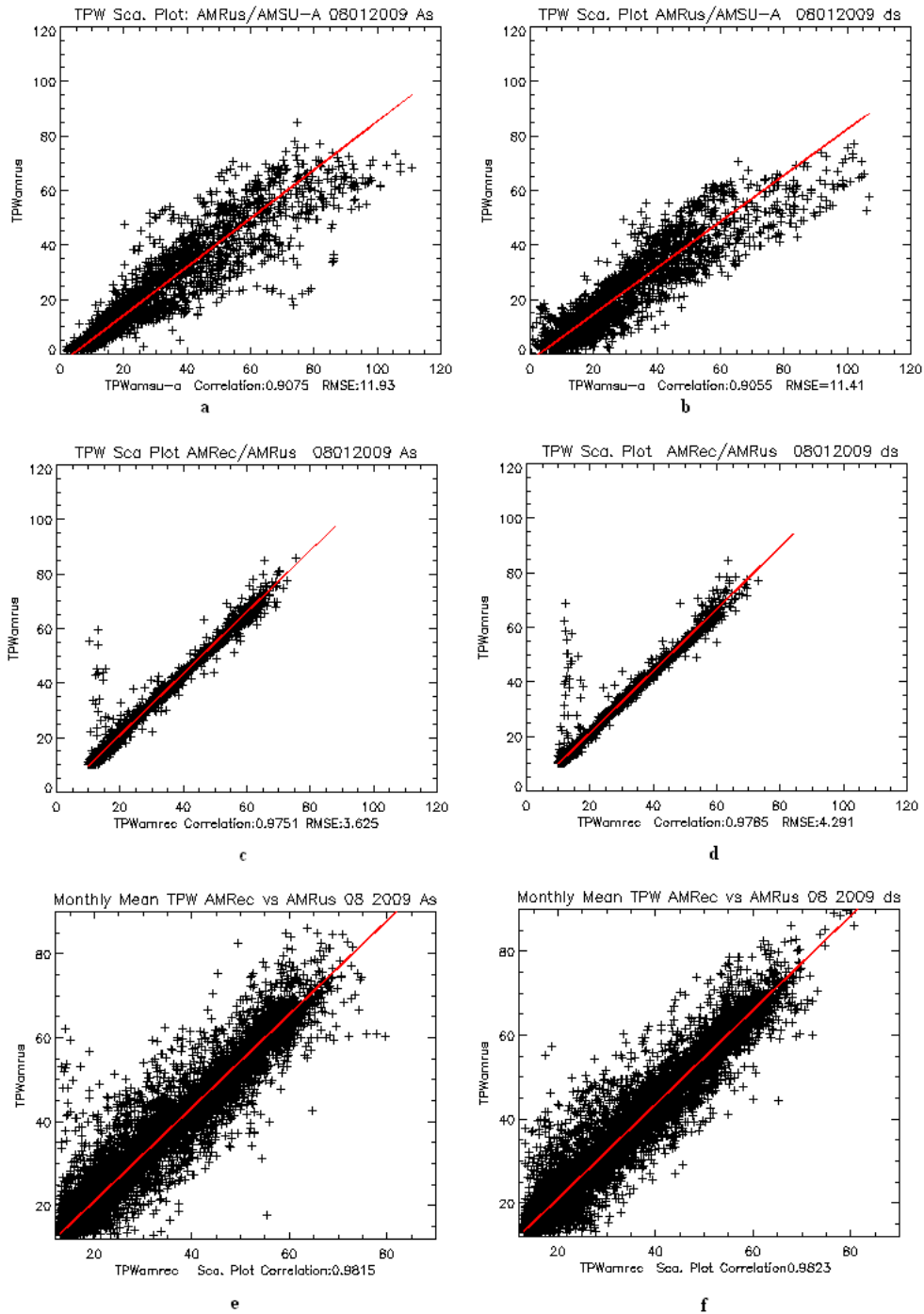


Figure 4 Daily TPW Correlations and RMSEs for 08012009: AMRus vs AMSU-A(a,b); AMRus vs AMRec (c,d)
 Monthly TPW Correlation between AMRus and AMRec for 08 2009 (e,f)

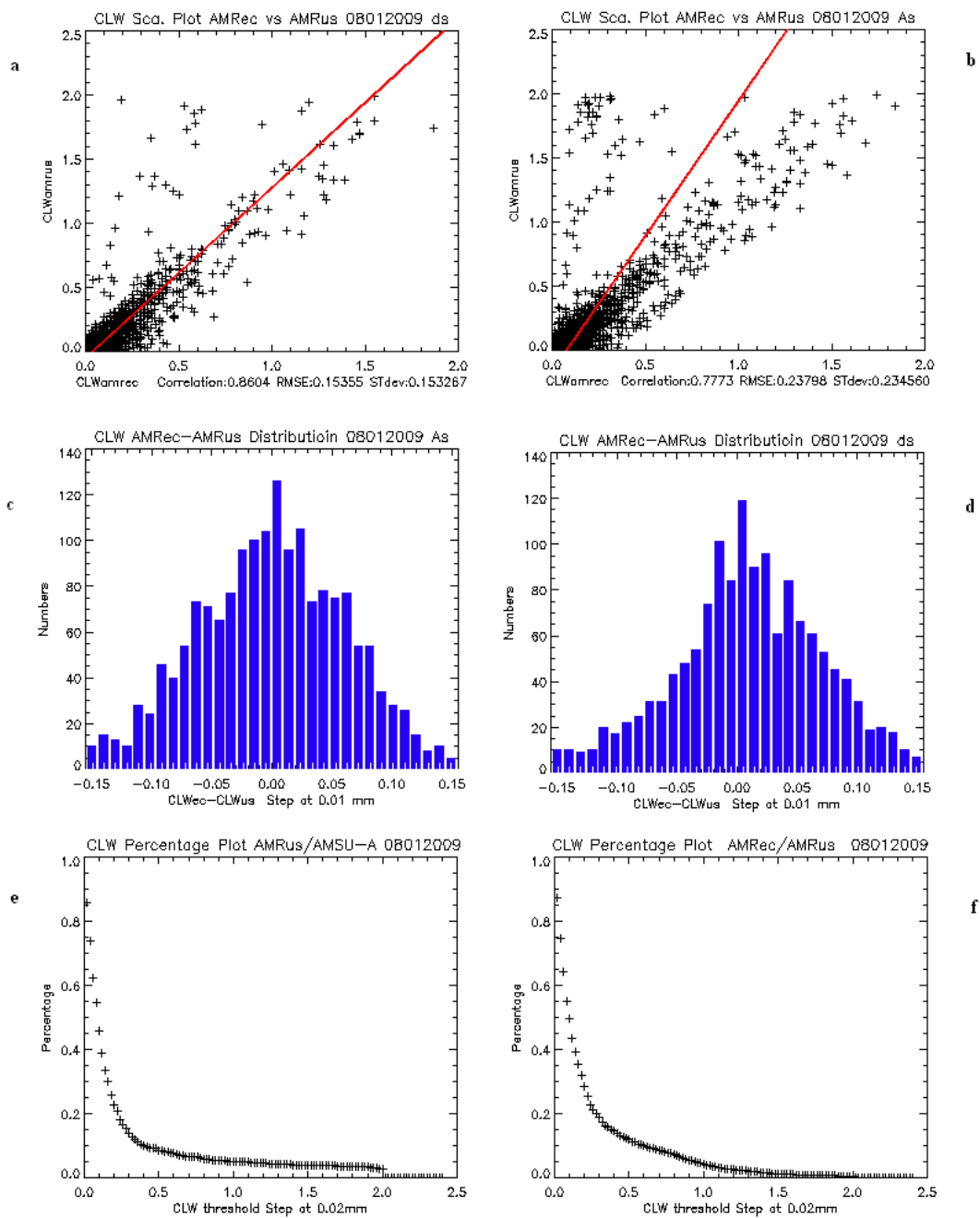


Figure 5 CLW Correlations and RMSEs between AMRus and AMRec for 08012009 (a,b)
 AMRec-AMRus CLW distribution for 08012009 (c,d)

CLW percentage between AMRus and AMSU-A (e) and CLW percentage between AMRec and AMRus (f):
 The X-axes is the cloud existence threshold from 0 to maximum CLW here at 2.5 mm. The Y-axis is the
 percentage of points where both retrievals are higher than the threshold with respect to all retrieved points for
 08012009.

References

Alishouse, J., S. Snyder, J. Vongsathorn, and R. Ferraro, 1990a: Determination of oceanic precipitable water from the SSM/I, *IEEE Trans. Geosci. Remote Sens.*, **28**, 811–816.

Alishouse, J., Snider, E. Westwater, C. Swift, C. Ruf, S. Snyder, J. Vongsathorn, and R. Ferraro, 1990b: Determination of cloud liquid water content using the SSM/I, *IEEE Trans. Geosci. Remote Sens.*, **28**, 817–822.

Bernstein, B.C., F. McDonough, M. K. Politovich, B. G. Brown, T. P. Ratvasky, D. R. Miller, C. A. Wolff, G. Cuning, 2005: Current Icing Potential: Algorithm Description and Comparison with Aircraft Observations. *Journal of Applied Meteorology* **44**:7, 969-986.

Cao, C., P. Ciren, M. Goldberg, F. Weng, 2005, Inter-satellite calibration of HIRS from 1980 to 2003 using the simultaneous nadir overpass (SNO) method for improved consistency and quality of climate data, resented at the ITSC14, Beijing, May 2005.

Cober, S.G., A. Tremblay and G.A. Issac, 1996: Comparisons of SSM/I Liquid Water Paths with aircraft measurements. *J.Geophys. Res.*, **101D**,503-519.

Deblonde, G., and N. Wagneur, 1997: Evaluation of global numerical weather prediction analysis and forecasts using DMSP special sensor microwave imager retrievals, *J. Geophys. Res.*, **102**, 1833–1850.

Desai, S.D., B.J. Haines, 2004: Monitoring measurements from the Jason-1 Microwave Radiometer and Independent validation with GPS, *J. Mar. Geod.* **27**, 221-240.

Ferraro, R.R., F. Weng, N. Grody, and A. Basist, 1996: An eight year (1987-1994) time series of rainfall, clouds, water vapor, snow and sea ice derived from SSM/I measurements, *Bull. Amer. Meteor. Soc.*, **77**, 891-905.

Greenwald, T., G. Stephens, T. Vonder Haar, and D. Jackson, 1993: A physical retrieval of cloud liquid water over the global oceans using

Special Sensor Microwave/Imager (SSM/I) observations, *J. Geophys. Res.*, **98**, 18,471–18,488.

Grody, N., J. Zhao, R. Ferraro, F. Weng and R. Boers, 2001: Determination of precipitable water and cloud liquid water over oceans from the NOAA 15 advanced microwave sounding unit. *J. Geophys. Res.*, **106 D3**, 2943–2953.

Guan, H., S. G. Cober, and G. A. Isaac, 2001: Verification of supercooled cloud water forecasts with in situ aircraft measurements. *Wea. Forecasting*, **16**:145–155.

Guan, H. Stewart G. Cober, George A. Isaac, André Tremblay, André Méthot, 2002: Comparison of Three Cloud Forecast Schemes with In Situ Aircraft Measurements. *Weather and Forecasting* **17**:6, 1226-1235.

Han, Y., and E. R. Westwater, Remote sensing of tropospheric water vapor and cloud liquid water by integrated ground-based sensors, *J. Atmos. Oceanic Technol.*, **5**, 1050–1059, 1995.

Jackson, D. L., and G. L. Stephens, 1995: A study of SSM/I-derived columnar water vapor over the global oceans, *J. Clim.*, **8**, 2025–2038.

Kokhanovsky, A.A., V. V. Rozanov, T. Nauss, C. Reudenbach, J. S. Daniel, H. L. Miller, and J. P. Burrows, 2006: The semianalytical cloud retrieval algorithm for SCIAMACHY I, 2006: The validation. *Atmos. Chem. Phys.*, **6**, 1905–1911.

Liu, G., and J.A. Curry, 1993: Determination of Characteristic Features of Cloud Liquid Water From Satellite Microwave Measurements. *J. Geophys. Res.*, **98D3**, 5069-5092.

Norman G., J. Zhao, R. Ferraro, F. Weng, and R. Boers, 2001: Determination of precipitable water and cloud liquid water over oceans from the NOAA 15 advanced microwave sounding unit. *J. Geophys. Res.*, **106D3**, 2943-2953.

Prat, R.W., 1985: Review of radiosonde humidity and temperature errors. *J. Atmos. Oceanic Technol.*, **2**, 404-407.

Scharroo, R., J. L. Lillibridge and W.H.F.Smith, 2004: Cross-Calibration and Long-Term Monitoring of the Microwave Radiometers of ERS, TOPEX, GFO, Jason, and Envisat. *J. Mar. Geod.* **27**, 279-297.

Solheim, F., J. R. Godwin, E. R. Westwater, H. Yong, S. J. Keihm, K. Marshand and R. Ware, 1998: Radiometric profiling of temperature, water vapor and cloud liquid water using various inversion methods. *Radio Science*, **33**, 393-404.

Tremblay, A., P. A. Vaillancourt, S. G. Cober, A. Glazer, G. A. Isaac, 2003: Improvements of a Mixed-Phase Cloud Scheme Using Aircraft Observations. *Monthly Weather Review* **131**:4, 672-686.

Trenberth, K. E., and C. J. Guillemot, 1995: Evaluation of the global atmospheric moisture budget as seen from analysis, *J. Clim.*, **8**, 2225–2272.

Vaillancourt, P.A., A Tremblay, S. G. Cober, G. A. Isaac, 2003: Comparison of Aircraft Observations with Mixed-Phase Cloud Simulations. *Monthly Weather Review* **131**:4, 656-671.

Wade, C.G, 1994: An evaluation of problems affecting the measurement of low relative humidity on the United States radio-sonde. *J. Atmos. Oceanic Technol.*, **11**, 687-700.

Weng, F., L. Zhao, R. Ferraro, G. Poe, X. Li, and N. Grody, 2003: Advanced Microwave Sounding Unit Cloud and Precipitation Algorithms. *Radio Sci.*, **38**, 8,086-8,096.

Weng, F., N. C. Grody and R. R. Ferraro and A. Basist and D. Forsyth, 1997: Cloud liquid water climatology derived from the Special Sensor Microwave Imager. *J. Climate*, **10**, 1086-1098.

Weng, F., and N. Grody, 1994a: Retrieval of cloud liquid water using the Special Sensor Microwave Imager (SSM/I), *J. Geophys. Res.*, **99**, 25,535–25,551.

Weng, F., and N. C. Grody, 1994b: Retrieval of liquid and ice water content in atmosphere using the special sensor microwave imager (SSM/I), *Microwave Radiometer and Remote Sensing of Environment*, Ed. by Solminili, VSP, Netherlands, p. 281 - 295.

Wentz, F. J., 1997: A well-calibrated ocean algorithm for SSM/I. *J. Geophys. Res.*, **102**, 8703–8718.